Journal of Volcanology and Geothermal Research 186 (2009) 320–330

Contents lists available at ScienceDirect

Journal of Volcanology and Geothermal Research

journal homepage: www.elsevier.com/locate/jvolgeores

Morphometry of scoria cones located on a volcano flank: A case study from Mt. Etna (Italy), based on high-resolution LiDAR data

Massimilano Favalli [a,*], Dávid Karátson [b,c], Francesco Mazzarini [a], Maria Teresa Pareschi [a], Enzo Boschi [a]

[a] Istituto Nazionale di Geofisica e Vulcanologia, via della Faggiola 32, I-56126 Pisa, Italy
[b] Department of Physical Geography, Eötvös University, Pázmány s. 1/c, H-1117 Budapest, Hungary
[c] Geoscience Center, University of Göttingen, Goldschmidtsrasse 1, 37077 Göttingen, Germany

ARTICLE INFO

Article history:
Received 4 February 2009
Accepted 21 July 2009
Available online 29 July 2009

Keywords:
scoria cone
morphometry
Etna
H/W_{co} ratio
DEM analysis

ABSTRACT

By using new high-resolution (2 m) digital elevation model derived from the 2005 LiDAR survey of Mt. Etna volcano (Italy), our study measured the classical morphometrical parameters for scoria cones, i.e. W_{co} (cone width), W_{cr} (crater diameter), H (cone height) as well as volume, inclination of cone slope and substrate, and a number of other parameters for 135 scoria cones of Mt. Etna. Volume and age distribution of cones shows that there is no direct structural control on their emplacement in terms of Etna's rift zones. The cones are progressively smaller in size toward summit, which can be explained by the large volcano's feeding system and progressively frequent lava burial toward top.

A careful analysis of H/W_{co} ratio (determined as 0.18 for other volcanic fields worldwide) shows that this ratio strongly depends on (1) the calculation method of H and (2) lava burial of cone. For Etnean cones, applying an improved method for calculating H relative to the dipping substrate results in a significantly lowered standard H/W_{co} ratio (0.137), which in turn questions the validity of the classical value of 0.18 in the case of large central volcanoes. The reduction of the ratio is not only due to methodology but also to the common lava burial. This can be expressed even better if H_{mean} is used instead of H_{max} ($H_{mean}/W_{co} = 0.098$). Using this measure, at Etna, well formed cones have higher ratios than structurally deformed (e. g. double or rifted) cones.

Furthermore, although the sampled scoria cones at Etna have formed in a relatively narrow time interval (<6500 yrs BP), there is a slight decrease in H/W_{co} corresponding to erosional changes detected globally ($H/W_{co} = 0.143$, 0.135 and 0.115 for three age classes of Etna's scoria cones, corresponding to average slopes of 26.6, 23.9 and 23.7°). Because the morphometrical effect of position on a dipping substrate as well as lava burial exceeds the effect of erosion, we call attention to use caution in simply using the H/W_{co} ratio of scoria cones for detecting age, especially on large active volcanoes.

© 2009 Elsevier B.V. All rights reserved.

1. Introduction

Scoria cones are the most common and most uniform volcanic landforms as demonstrated in previous key papers of Porter (1972), Settle (1979) and Wood (1980a,b). Due to the great number of such cones in large monogenetic volcanic fields (typically developed on flat areas and associated with a single or a few more silicic, voluminous volcanic centres; Connor and Conway, 2000), they provide a good opportunity for quantitative morphometrical studies (e.g. Scott and Trask, 1971; Porter, 1972; Bloomfield, 1975; Settle, 1979; Wood, 1980a, b; Martin del Pozzo, 1982; Hasenaka and Carmichael, 1985; Moriya, 1986; Tibaldi, 1995).

In most of these studies, standard morphometric parameters H (cone height), W_{co} (cone width) and W_{cr} (crater width) were used. Based on these parameters, Porter (1972) was the first to conclude that H/W_{co} is constant (~0.18) for a great number of Hawaiian (Mauna Kea) cones, a relationship that has later been confirmed and further supported by many examples worldwide (e.g. San Francisco Volcanic Field, Arizona, Wood 1980a; Paricutin and Michoacán-Guanajuato fields, Mexico, Hasenaka and Carmichael, 1985; Nunivak Island, Alaska, Settle, 1979; Etna, Italy, Settle, 1979; Fuji, Japan, Moriya, 1986). Settle (1979) and, in more detail, Wood (1980b) also demonstrated that H/W_{co} decreases with time due to erosion. For old (some Ma) scoria cones especially under arid–semiarid climates, where linear erosion is limited, areal redistribution of scoria (i.e. lowering of cone and enlargement of basal diameter) results in a progressively smaller H/W_{co} ratio down to 0.08 (Wood, 1980b; Hooper and Sheridan, 1998).

These examples of scoria cones studied by previous authors are located mostly on a flat surface (monogenetic volcanic fields), but they can also be found on gently to moderately dipping planes (large volcano flanks: Mauna Kea, Hawaii; Etna, Italy; Mt. Cameroon,

* Corresponding author.
E-mail address: favalli@pi.ingv.it (M. Favalli).

0377-0273/$ – see front matter © 2009 Elsevier B.V. All rights reserved.
doi:10.1016/j.jvolgeores.2009.07.011

Cameroon; Nyiragongo, Democratic Republic of Congo, etc.). The slope of the flank can have a considerable effect on the emplacement of a cone. For example, Tibaldi (1995) pointed out that the direction of crater breach is strongly controlled by the substrate slope dip if its inclination is >9°.

However, none of the above authors focussed on the geometrical consequences to H, W_{co} and their ratio in the case of emplacement on a volcano flank. There are at least two problems to be addressed: (1) how to calculate the (relative) height of the scoria cone on a dipping plane, and (2) what are the morphometrical consequences of burial by subsequent, regular lava overflows.

In this paper we investigate the scoria cone field of Mt. Etna volcano by using new (September 2005) high-resolution LiDAR data, interpolated on a 2 m stepped DEM (Favalli et al., 2009). The Etnean cones are located from 400 m to higher then 3000 m a.s.l. on a large central volcano having variously dipping flanks (Fig. 1). Although these cones are all Holocene in age, their morphology, in most cases, has been significantly modified by the subsequent effusive activity of Etna, and to a less extent by erosion (related to the high altitude and the Mediterranean climate). All these factors result in significant changes of cone shape that may be detected by high-resolution morphometry.

2. Geological background of Etna's flank eruptions

Mt. Etna volcano, located on the east coast of the island of Sicily, Italy, has a basal diameter of about 40 km and an elevation of about 3350 m. It evolved on the continental crust of eastern Sicily at the tectonic boundary marked by the subducting Ionian oceanic slab (Gvirtzman and Nur, 1999). Its structural dynamics are principally characterized by volcanic spreading, which results in an overall seaward movement of its eastern sector, accomplished mostly by movements along fault systems bordering this mobile portion (e.g. Borgia et al., 1992; Monaco et al., 1997; Froger et al., 2001; Lundgren et al., 2004; Catalano et al., 2004).

The geology of Etna is dominated by lava flows with subordinate pyroclastic and epiclastic deposits (Chester et al., 1985). In the late Pleistocene, the activity of Mt. Etna was close to its present summit area, generating the Ellittico Volcano characterized by a wide summit caldera that collapsed about 14 ka BP (Branca et al., 2004 and references therein). The Ellittico Caldera has been almost completely buried by later products of the Recent Mongibello volcanic activity (Romano et al., 1979; Branca and Del Carlo, 2004). The Recent Mongibello volcanic activity has been characterised by almost continuous eruptions of effusive and moderate explosive activity (e.g. Calvari et al., 2002;

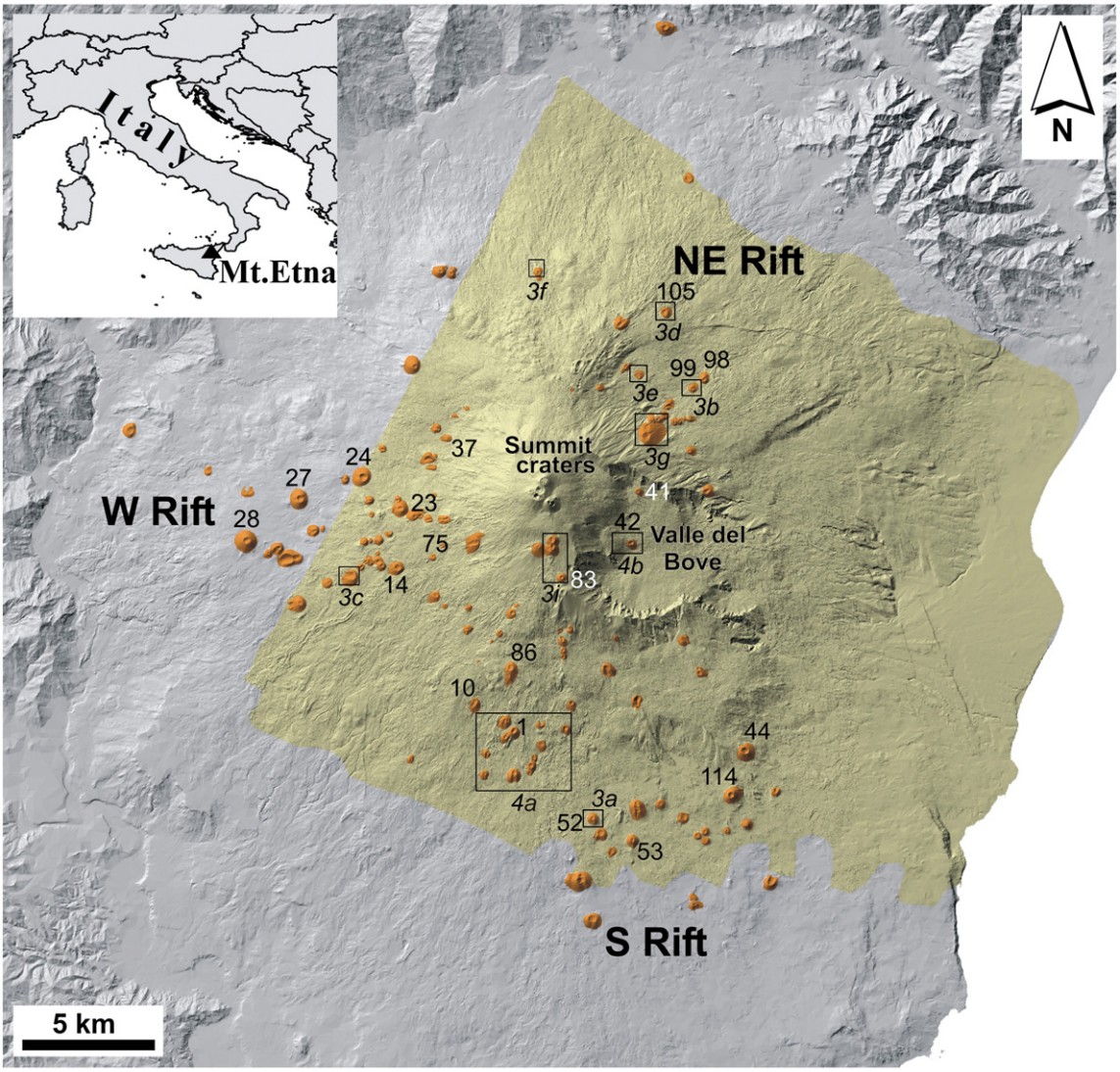

Fig. 1. Shaded relief image of Mt. Etna digital elevation model (DEM). Illumination from the northwest. For our morphometrical study, topographic data of the 2 m-stepped DEM of the 2005 LiDAR survey (Favalli et al., in print, yellow area), whereas outside the 10 m-resolution DEM derived from the 1998 Mt. Etna aereophotogrammetrical data was used (Tarquini et al., 2007). The scoria cones considered in this paper are brown-coloured. Boxes show the locations in Figs. 3 and 4. Numbers indicate individual examples (Table 2).

Table 1
Morphometrical parameters used in the paper.

Parameter	Unit	Description
ID		Numerical cone identifier
X	m	*X* location (WGS84, UTM zone 33N) of the baricenter of the polygon enclosing the base of the cone
Y	m	*Y* location (WGS84, UTM zone 33N) of the baricenter of the polygon enclosing the base of the cone
Z_min	m	Minimum elevation a.s.l. of the cone surface
Z_max	m	Maximum elevation a.s.l. of the cone surface
Z_average	m	Average elevation a.s.l. of the cone surface
DISTANCE	m	Distance of the cone from the summit craters ($x=499{,}464$; $y=4{,}178{,}246$; WGS84, UTM zone 33N)
AZIMUTH	degree	Azimuth of the position of the cone relative to summit craters
AREA	m^2	Planimetric area of the cone
AREA_CR	m^2	Planimetric area of the crater of the cone
SLOPE	degree	Average slope of the flanks of the cone, calculated by averaging the slopes of grid points inside the base polygon and outside the crater polygon
VOLUME	m^3	Cone volume enclosed between the DEM surface and the 3D base surface defined as the Delaunay triangulation of the 3D points of the base polygon
H_{co}	m	Average cone height, calculated as the mean elevation of the 3D crater rim above the 3D base surface defined as above
*H*_max	m	Max cone height, calculated as the max elevation of the 3D crater rim above the 3D base surface
CRATER_DEPTH	m	Crater depth, calculated as the difference between the average cone height (*H*) and the minimum height inside the crater polygon
BP_SLOPE	degree	Slope of the basal plane. The basal plane is calculated as the plane best fitting to a ring region outside the base polygon and not overlapping base polygons of other cones: in this way this represents the real slope underlying the cone
BP_AZIMUTH	degree	Azimuth of the dip direction of the basal plane
D_min	m	Length of the minimum base diameter
D_max	m	Length of the maximum base diameter
AZI_D_min	degree	Azimuth (between 0 and 180) of the direction of the minimum diameter (D_MIN)
AZI_D_max	degree	Azimuth (between 0 and 180) of the direction of the maximum diameter (D_MAX)
L_min	m	Length of the minor diameter of the ellipse best fitting the base of the cone
L_max	m	Length of the major diameter of the ellipse best fitting the base of the cone
AZI_L_max	degree	Azimuth (between 0 and 180) of the direction of the major diameter (L_MAX) of the best fitting ellipse
W_{co}	m	Average diameter of the base of the cone calculated as $\sqrt{4\mathrm{AREA}/\pi}$
W_{cr}	m	Average diameter of the crater of the cone calculated as $\sqrt{4\mathrm{AREA\_CR}/\pi}$
AGE_CLASS		Class 1: cones younger than 122 BC, class 2: cones older than 122 BC, class 3: cones older than 5000 yrs BP (Alderigi, 1998 and references therein)
Zb_min	m	Minimum basal elevation a.s.l.
Zb_max	m	Maximum basal elevation a.s.l.
Zc_max	m	Maximum elevation a.s.l. of the crater rim
W_{co} (old)	m	Basal diameter of the cone calculated as the average of the maximum and minimum base diameters
H_{co} (old)	m	Cone height calculated as the difference between the maximum elevation of the cone rim and the average basal elevation

Behncke and Neri, 2003; Andronico et al., 2005; Mazzarini et al., 2005; Allard et al., 2006). The present summit area of Mt. Etna consists of four main eruptive centres (Bocca Nuova, Voragine, and NE and SE cones). Several eruptions have occurred from both summit and flank vents (Romano et al., 1979; Romano and Sturiale, 1982; Branca and Del Carlo, 2004), producing numerous composite lava fields (e.g., Rittmann, 1973; Romano, 1982; Acocella and Neri, 2003) and more than 300 scoria and spatter cones. Additional information about historical eruptions of Mt. Etna, along with a daily update of its activity, is available on the Catania INGV website (http://www.ct.ingv.it/).

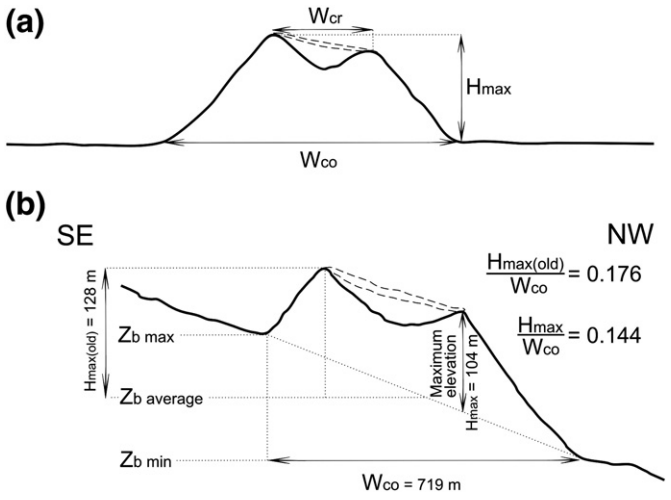

Fig. 2. Methods to calculate *H* and W_{co} of scoria cones. a) The classical method of Settle (1979) defines H_{max} as the maximum elevation above the average basal elevation of cone. b) In our improved method, H_{max} is the maximum elevation above the fitting basal plane. The example is a real cone (No. 24, see Fig. 1). The two methods give significant difference in the case of a dipping plane. Z_b: elevation of the cone base a.s.l.

The scoria cones of Etna's flanks (McGetchin et al., 1974; Settle, 1979; Villari et al., 1988; Mazzarini and Armienti, 2001; Corazzato and Tibaldi, 2006) cluster in three main sectors corresponding to the NE, S and W rift zones (Rittmann, 1973; Kieffer, 1975; Villari et al., 1988; Garduno et al., 1997; Mazzarini and Armienti, 2001). The cones grew on the Recent Mongibello and younger products (Romano et al., 1979). Their known age spans from prehistoric (ca. 6500 yrs dated cones) to historical times, and the most recent scoria cones, southward of the SE crater, were built up in 2002–2003 (Romano et al., 1979; Romano and Sturiale, 1982; Coltelli et al., 1995; Alderigi, 1998; Coltelli et al., 1998; Del Carlo and Branca, 1998; Behncke and Neri, 2003; Branca and Del Carlo, 2004; Corazzato and Tibaldi, 2006; Tanguy et al., 2007). A very important marker in the Recent Mongibello stratigraphy is the occurrence of a Plinian deposit of Roman age (122 BC: Coltelli et al., 1998). It covered many scoria cones and, therefore, is useful for rough division between old and historical cones.

The young ages of Etnean scoria cones included in this study imply a morphologically homogenous population; the time span of their formation is much smaller than that of most other studied scoria cone fields either on a flat surface (e. g. San Francisco Volcanic Field: <5 Ma, Hooper and Sheridan, 1998) or a large volcano (e.g. Mauna Kea, Hawaii: <0.3 Ma, Settle, 1979).

3. Methodology

3.1. The high-resolution DEM of Etna

Airborne altimetric LiDAR (Light Detection and Ranging) data have been used to generate a high-resolution (2 m step) digital elevation model (DEM) of most of Mt. Etna flanks from data acquired during a LiDAR survey at Mt. Etna in September 2005 (Favalli et al., 2009). The

LiDAR survey consists of more than 2.57×10^8 scattered topographic points. The points are distributed in thirty-four NNE–SSW trending strips covering most of our study area, i.e. a large part of Etna's northern, western and southern flanks and the majority of its eastern flanks (Fig. 1). The area covered by the survey is 616 km^2 large. By interpolating the scattered elevations a DEM of 2 m step was derived. The resulting DEM, geocoded to a UTM-WGS 84 projection, has an elevation accuracy of ± 0.4 m and a horizontal accuracy of ± 2.4 m. The accuracy was calculated following the procedure of Favalli et al. (2009) in which the errors are evaluated on the basis of distortions in the areas of overlap among the different strips collected during the survey. Outside the area covered by the LiDAR data, we have used a 10 m-step grid (updated in 1998, Tarquini et al., 2007) obtained by interpolating aerophotogrammetric contour lines and spot heights using DEST, an algorithm that reconstructs DEMs from sparse data in an unbiased way (Favalli and Pareschi, 2004).

3.2. Morphometric parameters

To date, standard parameters of scoria cone morphometry have typically been obtained as single values from topographic maps sometimes confirmed by aerial photos, giving some uncertainty and irreproducibility to the results. In one of the first comprehensive papers, Settle (1979), by using topographic maps of 1:25,000 to

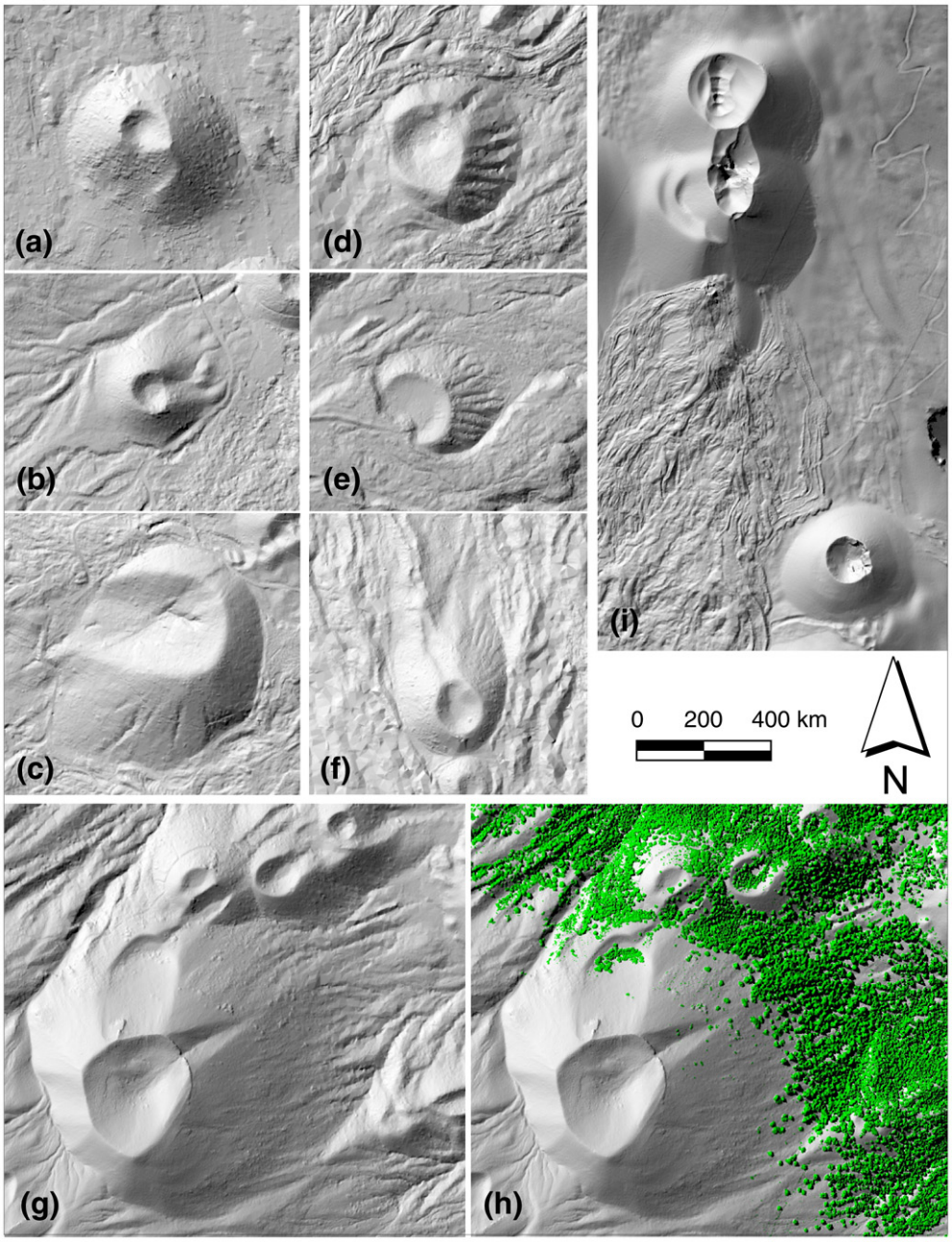

Fig. 3. Examples of Etnean scoria cones showing typical shape variations. (a) An old (pre-122 BC) "well formed" cone: the more than two thousand year-long period has not been enough to modify its perfect shape. (b) A less regular cone: the cone shape is obvious, but the base is irregular, so we did not include such features in the category of "well formed". (c) The majority of Etnean cones are even more poorly formed: although the single cone shape can be clearly recognised, the base tends to be irregular mostly due to lava burial. (d, e) Strongly eroded cones: if there is a well-developed gully system, we term these "heavily dissected cones". These features are infrequent on Etna due to common lava burial that covers and eventually buries the cones. (f) Many cones show only a little sign of gully dissection. (g, h) Example of how gully formation is controlled by vegetation, that in turn is related to altitude and exposure. (i) Cone shape can change during emplacement due to eruptive dynamics, a frequent category we term "structurally deformed cone". Good examples are the youngermost double cones of Etna (2002–2003, above), whereas the 2001 single cone (below) is "well formed".

1:62,000 scale, defined W_{co} as "the average (mean) of the maximum and minimum base diameters". The classical papers of Porter (1972) and Wood (1980a,b) were also based on this method, and according to our survey, all the other subsequent papers, referred to above, calculated W_{co} this way. By using this definition, or even by calculating the average of 4 or 8 diameters, we can get reliable results for circular/

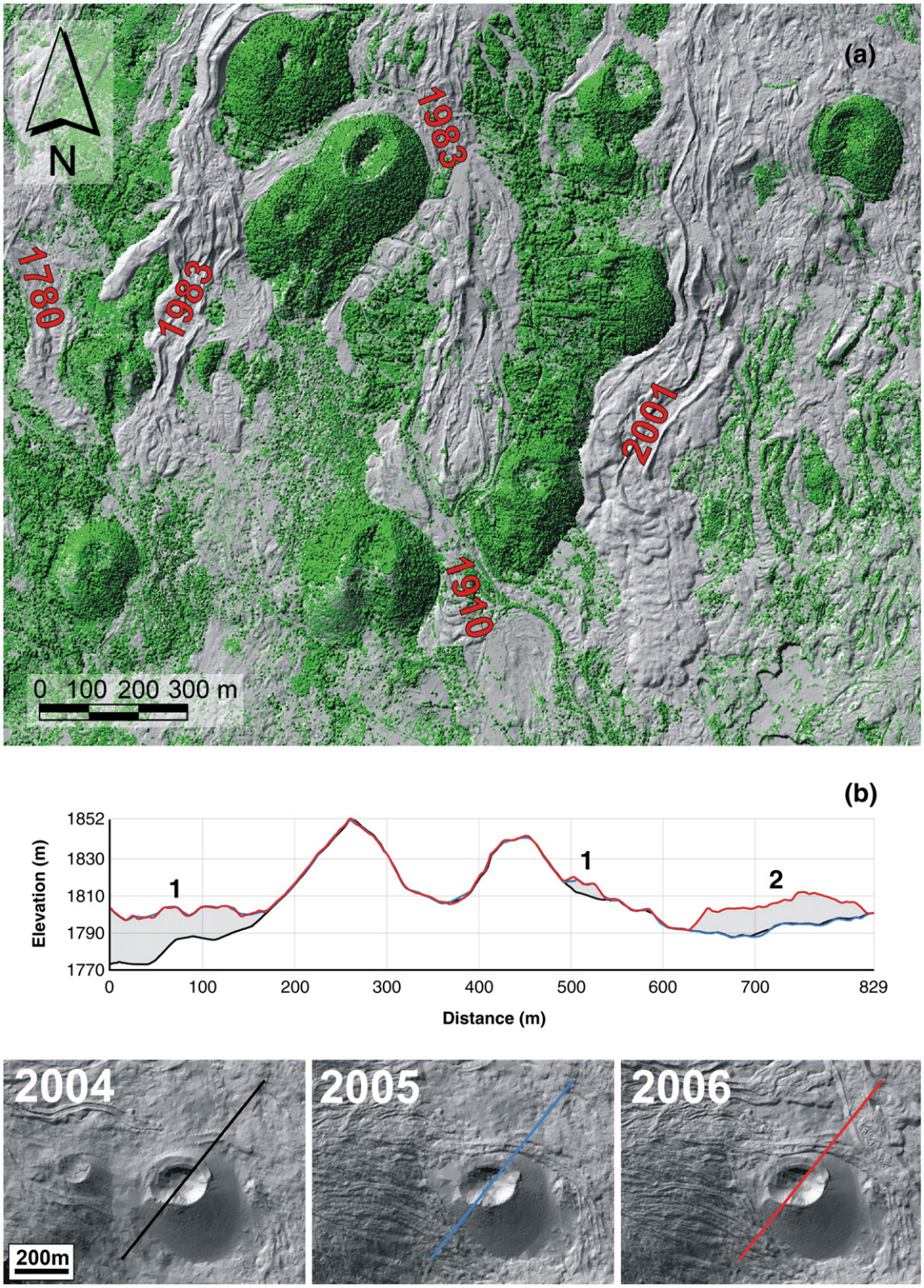

Fig. 4. (a) Forested scoria cones surrounded by historical to recent lava flows in between on 2-m-resolution shaded relief DEM, showing the effect of lava flow to reduce relative height of cones. (b) Topographic profile (vertical exaggeration 2×) and shaded relief images of a selected area in Valle del Bove, covered by 2004–2006 lavas (see Fig. 1) on 3 different Laser scanning DEMs of Mt. Etna. Black line refers to the September 2004 survey, blue line to the September 2005 survey and red line to the November 2006 survey. In the profile, 1 labels the lava accumulated during 2004–2005, whereas 2 that of the 2006 eruption. (For interpretation of the references to colour in this figure legend, the reader is referred to the web version of this article.)

elliptical cones. However, for irregular-shaped cones, results will largely depend on where to measure the diameter. Here, benefitting from the high-resolution DEM, as a first step we used the detailed shaded relief image and a derivative slope map to outline the contours of each cone and crater. Then, starting from the resulting base polygons, crater rim polylines and crater polygons, the standard morphometric characteristics have been calculated with the help of a C++ program developed ad-hoc. This way, W_{co} could be obtained by more precise areal-type data (see Table 1). In the calculation, we used the planimetric projection of the cone basal area (see Fig. 2), because,

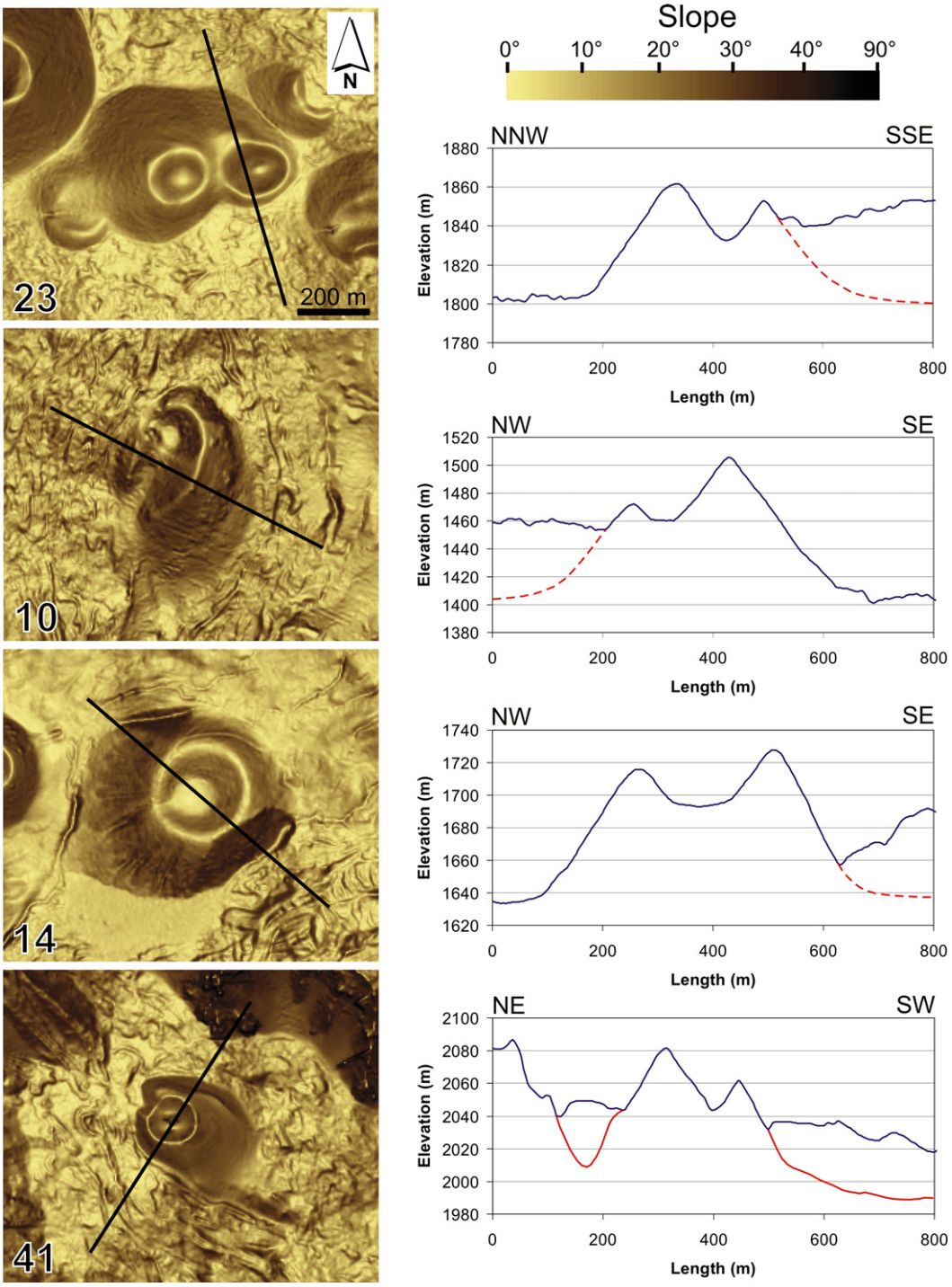

Fig. 5. Selected scoria cones of Etna on a derivative slope map of the 2-m DEM showing the effect of lava cover on morphology. Real present profiles (continuous blue line) are completed by real (continuous red line) or hypothetic (dashed red line) previous ones. Cones are numbered according to their ID (see Table 1). For locations, see Fig. 1. (23) A superposed, intact, well formed cone, elongated downslope on Etna's flank, the eastern part being almost completely inundated by lava flow. (10) A breached, elongated double cone, its W part and crater rim being partly buried by lava. (14) A well formed, although slightly dissected cone, possibly with its SE sector collapsed due to lava flow. (41) A cone almost completely surrounded by lava. The continuous red line is the profile on the 1998 DEM (Tarquini et al., 2007). The surface morphology of the cone is completely changed due to the lava that flowed it around: cone height, for example, reduced to one half. (For interpretation of the references to colour in this figure legend, the reader is referred to the web version of this article.)

for the Etnean flanks <20°, the result would differ by only <4% if calculated from the real 3D cone basal area.

We have found the measurement of H even more problematic. Settle (1979) defined this parameter "as the difference between the average basal elevation and the maximum elevation observed at the cone's rim crest or summit" (Fig. 2). All subsequent papers used this method to calculate H (see Hooper and Sheridan, 1998, and references therein). Selecting the highest point on the rim and comparing it to the average basal elevation gives reliable result in the case of flat or gently dipping basal plane. However, as Fig. 2 demonstrates, if we have a considerably dipping plane, we will obtain spurious results: as an example from Etna's western flank testifies, the height we measure by using the classical method far exceeds the greatest elevation above the basal plane. Based on Fig. 2 and the above definition of W_{co}, in our work we measured H as the elevation above the fitted cone basal plane. Furthermore, although measuring the maximum elevation of cone has been a standard in all previous works, in addition we also calculated the cone mean elevation provided by the high-resolution DEM (i.e. mean elevation of crater rim above the basal plane).

In Table 1, we provide the definition of all the parameters we measured for the Etnean scoria cones. Benefitting from the obtained areal-type data (i.e. cone surface and basal plane), for the first time we also calculated cone volume, a parameter that could not be obtained reliably from topographic maps.

3.3. Classification of Etnean scoria cones

The high-resolution shaded relief map of Etna reveals various types of scoria cones (Fig. 3). Out of the 135 studied cones, a large number of cones have an intact, regular shape. However, many of them are moderately or strongly modified by syn- and post-emplacement processes. The syn-emplacement processes, resulting from peculiar eruptive dynamics, include morphostructural effects that produce multiple cones, coalescent cones, rifted cones, lava-flow breached or slumped cones (e.g. Corazzato and Tibaldi, 2006). We collectively term these "structurally deformed cones". The scoria cones not affected by these changes can also have various shape from regular to irregular, making it possible to distinguish "well formed cones", i.e. those having a regular cone shape.

The post-emplacement changes of a cone are mostly related to burial by lava flows. Although Porter (1972) and Wood (1980a) already mentioned that lava flows covering the surrounding terrain or a part of the cone may result in morphometrical changes, no authors examined this phenomenon on a quantitative basis. Lava flow burial, quite visible on the high-resolution DEM of Etna (Figs. 4 and 5), has been highly focussed in our study. In addition to this, some of the apparently oldest cones have been significantly affected by erosion, namely, dissection by gullies (Fig. 3). Therefore we have also distinguished "heavily dissected cones".

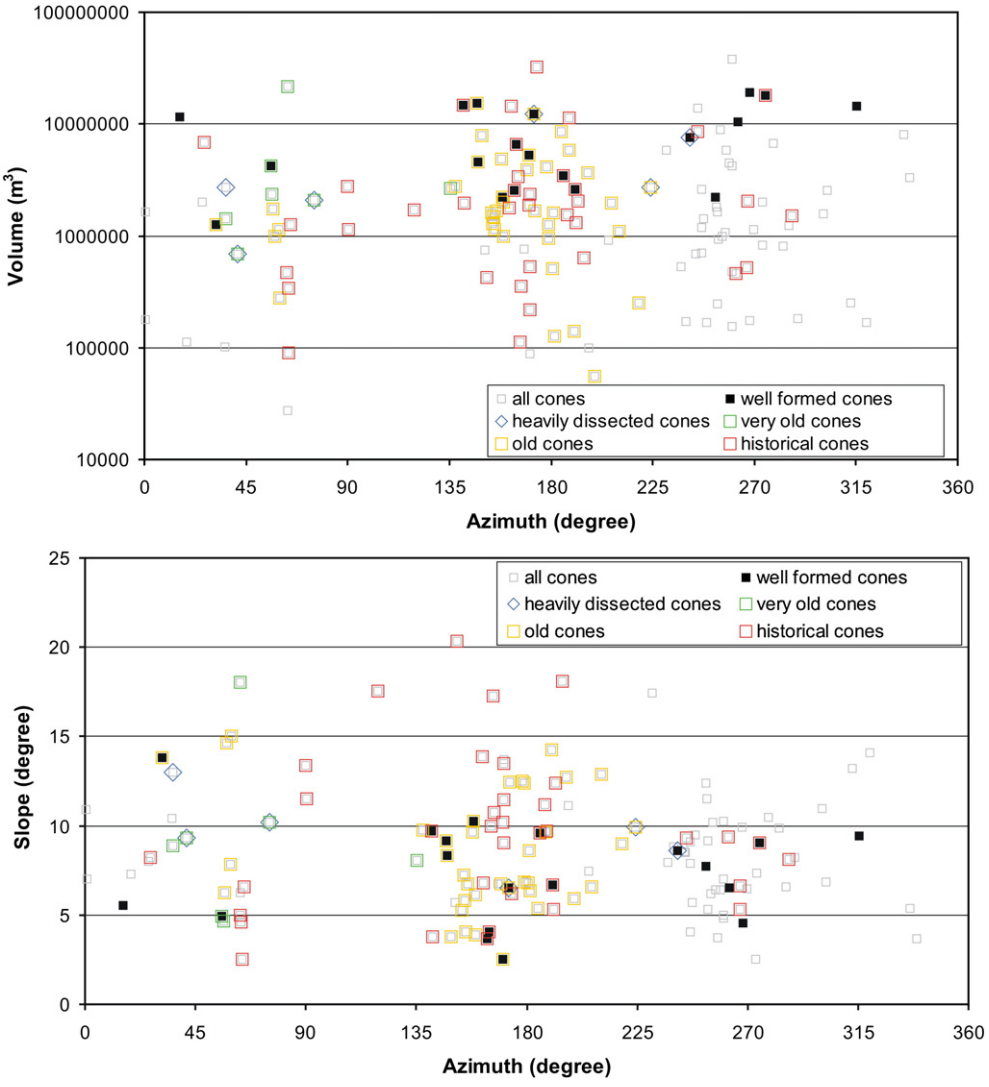

Fig. 6. Cone volume vs azimuth and average slope of basal plane vs azimuth plots for Etna's scoria cones.

Finally, according to the available age constraints (see references in Section 2), 80 scoria cones have been classified in terms of age. Three main age classes have been created. Historical cones include 36 cones (class 1) younger than 122 BC; 44 cones are older than 122 BC; within this, "old cones" (37, class 2) are those which have no further age constraints, and "very old cones" (7, class 3) are those older than 5000 yrs BP (Alderigi, 1998 and references therein).

4. Results

In accordance with the list of morphometric parameters in Table 1, all the obtained data are presented in the Supplementary Table. Using the data base, a number of plots, both standard and new, have been constructed.

In Fig. 6, volume and average slope of basal plane of scoria cones vs azimuth (i.e. geographic position on Etna's flank) are plotted, also displaying the shape and age classes we established. Large cones (>1,000,000 m^3) tend to be well formed, and are located on relatively gentle-sloped (<10°) basal planes, that is, on the lower flanks of Etna.

The standard H/W_{co} ratios of Etna's scoria cones differ from each other according to the above described calculation methods (Fig. 7). By using the classical method (Settle, 1979), the H/W_{co} ratio for Etnean cones (0.175; Fig. 7a) is close to the ideal 0.18 defined by Porter (1972) and Wood (1980a). However, by using our improved method for H (i.e. above the fitted basal plane), the ratio is much smaller (0.137; Fig. 7b). If we calculate with H_{mean}, the ratio becomes even more reduced (0.098; Fig. 7c).

Fig. 8 is the H/W_{co} plot using our improved method (calculating with H_{max}, that is, identical to Fig. 7b) and displaying the classifications by shape and age. As Fig. 8a shows, there is a significant difference between well formed cones ($H/W_{co}=0.158$) and structurally deformed cones ($H/W_{co}=0.123$). The H/W_{co} ratio vs age classes (Fig. 8b) also results in slight variations, that follow Wood's (1980b) rules on the reduction of the ratio with time: the youngest (historical) cones of Etna have the highest ($H/W_{co}=0.143$), the old cones have smaller ($H/W_{co}=0.135$), and the very old cones have the lowest ($H/W_{co}=0.115$) ratio, although the differences are small and the last value is statistically not so reliable due to the small number ($n=7$) in the class.

Finally, using H_{mean} instead of H_{max} and displaying well formed cones separately, in the H/W_{co} plot (Fig. 9) we find that the difference between well formed cones ($H/W_{co}=0.128$) and the total population ($H/W_{co}=0.098$) is even more pronounced.

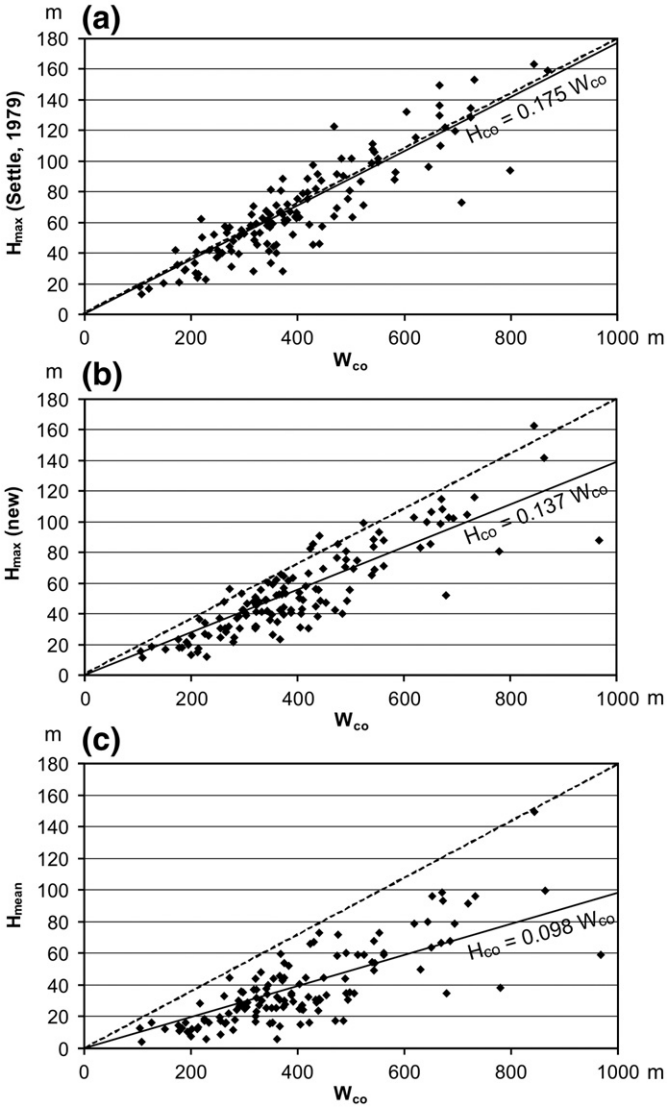

Fig. 7. H/W_{co} plots for Etna's scoria cones. (a) The standard H_{max} vs W_{co} plot by using Settle's (1979) method. (b) H_{max} vs W_{co} plot by using our improved definition for H. (c) H_{mean} vs W_{co} plot. The reference correlation line (dashed) corresponds to H/W_{co} 0.18 (Porter, 1972). For discussion, see text.

5. Discussion

Variations in cone volume and basal slope of Etna's scoria cones, as Fig. 6 testifies, have no direct relationship to their position in terms of rift zones. There is no relationship to ages either, although for the W rift, only a few age constraints are available. Given this uniformity, there is no reason to consider cone morphometry with respect to structural control. Apparently, volume is only controlled by elevation: with increasing altitude (i.e., steeper basal slope), cones tend to be smaller (see supplementary data). This may be due to two factors. (1) the main volcano's conduit system feeds progressively smaller cones toward the summit (i.e. radial eruptions sensu Romano and Sturiale, 1981). (2) the more frequent burial by lava flows of upper cones reduces their relative size. However, this latter factor can be assessed in a more direct way with the help of the H/W_{co} plots.

Fig. 7a–b clearly shows that, if a cone is emplaced on a steep basal plane, the H/W_{co} will be smaller than the value obtained by the classical method. The difference between the two H/W_{co} ratios on the average is 0.04, i.e. ~22%. Therefore, in the case of a scoria cone field located on a relatively steep volcano flank, we call attention on the importance of the method used to calculate H.

In order to see real examples showing this discrepancy, a number of Etnean cones, having gentle (2.5–5°) and steep (9–11°) basal planes, have been selected (Table 2). In fact, whereas cones emplaced on gentle slopes (Table 2a) can be characterized by similar or identical H/W_{co} ratios using either method, those emplaced on steep slopes (Table 2b) display contrasting H/W_{co} ratios.

The differences between H/W_{co} ratios can be further investigated in Fig. 8a, Fig. 9 and Table 2c. As Fig. 8a shows, well formed vs other cones show a big difference in H/W_{co}, which might be due to the fact that the poorer shaped cones (including the structurally deformed ones) are partly those covered by lava. Obviously, this process, reducing cone height, results in a lowered H/W_{co}. This is because, although lava overflow also decreases W_{co}, the reduction of H tends to 0, whereas the reduction of W_{co} cannot be smaller than W_{cr}, except total burial. A number of effects of lava overflow are illustrated in Figs. 4 and 5.

In Fig. 9, where H_{mean} is used, the more pronounced difference in H/W_{co} ratio can also be explained by lava burial. In this figure, the use of H_{mean} for regular, well formed cones (that are typically not inundated by lava) will result in a value close to H_{max}; on the contrary, for irregular-shaped (among others covered) cones, H_{mean} may be significantly reduced. This conclusion can be confirmed if

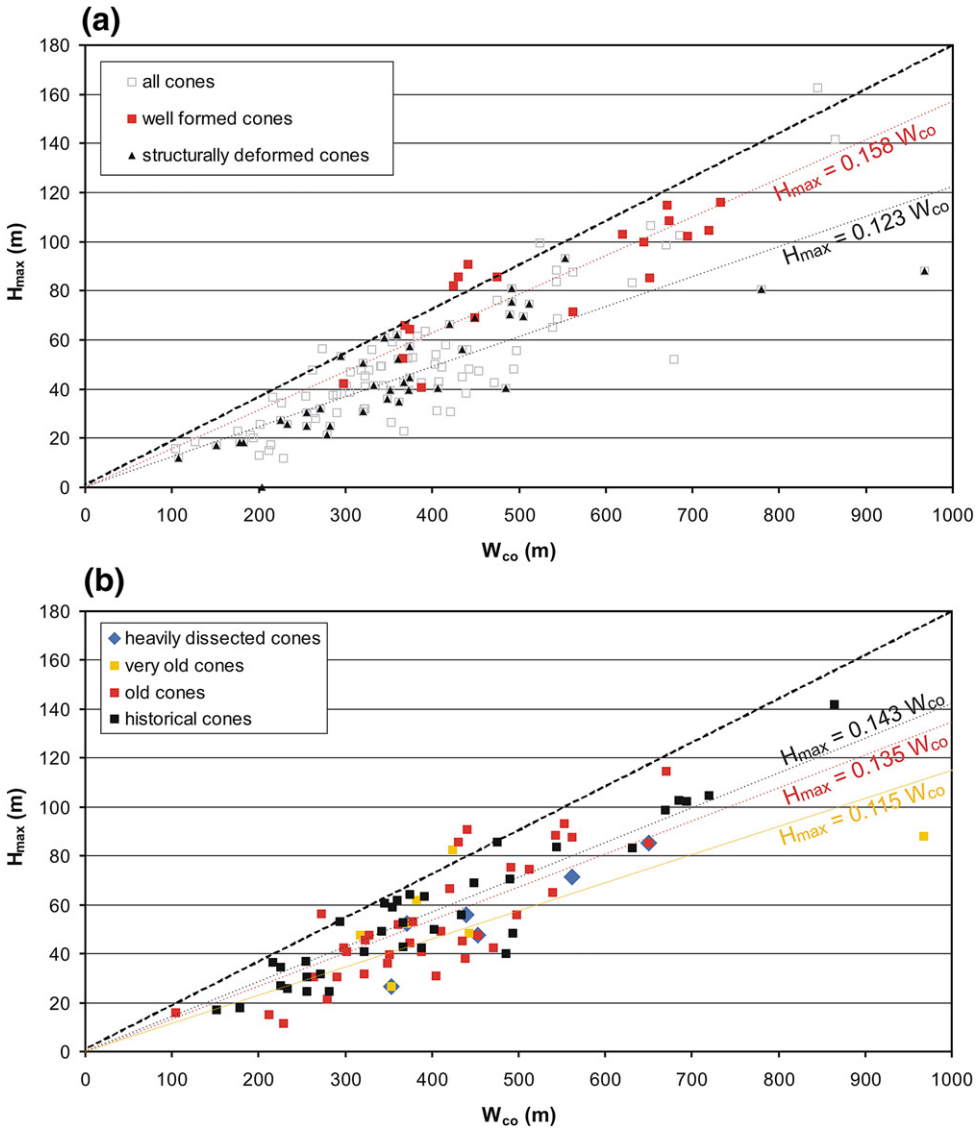

Fig. 8. H_{max} vs W_{co} plots of Etna's scoria cones (same as Fig. 7b) completed by categories of shape and age. (a) Plot distinguishing well formed and structurally deformed cones, (b) plot showing cones with age constraint. The black dashed line corresponds to H/W_{co} equal to 0.18 (Porter, 1972).

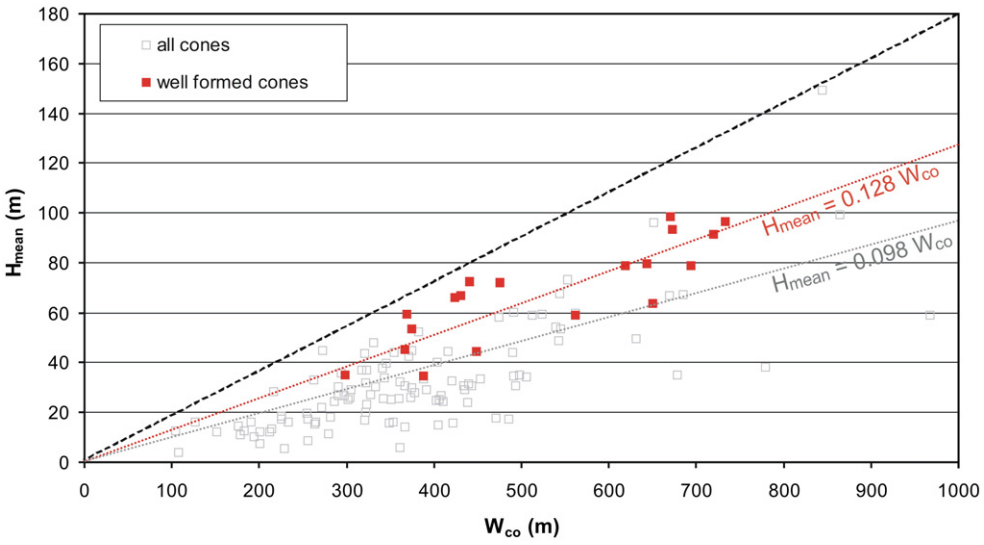

Fig. 9. H_{mean} vs W_{co} plot (same as Fig. 7c) distinguishing the well formed cones. The black dashed line corresponds to H/W_{co} equal to 0.18 (Porter, 1972).

Table 2
Morphometry of selected cones of Etna showing the differences between the classical (Settle, 1979) and our improved method to calculate H/W_{co}. Panel a includes cones located on gentle sloped (2.5–5°) basal plane, Panels b and c include those located on steep (9–17°) slopes. In addition, cones in Panel c have reduced height due to lava burial.

	Cone ID	H/W_{co} (Settle, 1979)	H/W_{co} (new)	Basal slope (°)
A	52	0.21	0.21	2.5
	83	0.22	0.17	3.7
	53	0.21	0.18	4.1
	27	0.19	0.16	4.6
	99	0.16	0.16	4.7
	28	0.19	0.19	4.9
	98	0.19	0.19	4.9
B	114	0.22	0.17	9.1
	1	0.20	0.15	9.6
	44	0.17	0.15	9.7
	86	0.21	0.15	9.7
	37	0.18	0.14	11.0
C	75	0.16	0.11	7.9
	105	0.19	0.13	13.0
	42	0.19	0.12	17.6

selecting cones unambiguously buried by lava and at the same time located on steep slopes (Table 2c): the differences will be even larger (0.05–0.07, 30–35%).

As put in the Introduction to this paper, lava burial is not the only factor reducing cone height. H/W_{co} ratios vs age classes (Fig. 8b) show a reduction by 0.03 (20%) in total. This means that, in spite of the short time span of formation of Etnean scoria cones, H is reduced relative to W_{co} with time. The reduction is in good agreement with results of previous studies (e. g., Wood, 1980b; Dohrenwend et al., 1986; Hooper and Sheridan, 1998; Riedel et al., 2003), although even the smallest ratio is far from the ones (<0.10) obtained for highly eroded several Ma old cones (e.g. San Francisco Volcanic Field).

That this reduction is related to erosion is further supported by morphometry. First, in Fig. 8b, the positions of cones dissected by gullies (for examples, see Fig. 3) are among those having the lowest H/W_{co} ratios. Second, if we correlate average slopes of cones with age classes, we find that the slope values are 26.6, 23.9 and 23.7° for age class 1, 2, 3, respectively. This way, if we do not have age constraint for a possibly old cone, a low H/W_{co} value plus the presence of intense gullying is a useful relative indicator of old age. We emphasize that, especially on steep slopes, using only H/W_{co} is not enough to infer the relative age (even if we use our improved method for H), because modification of H/W_{co} by lava burial gives equally big discrepancies.

6. Conclusions

In our work, 135 scoria cones of Etna were investigated by high-resolution morphometry. The flanks of Etna have various slopes up to ~20°, on which the scoria cones are scattered largely corresponding to the NE, W and S rift zones. However, as the volume, H/W_{co}, and age distributions of cones show, these parameters are uniform in the different zones, i.e. there is no direct structural control on them. On the other hand, smaller cones tend to occur toward the summit, probably in relation with the volcano's feeding system. Reduction of apparent size higher on the volcano is further enhanced by regular lava burial.

A detailed analysis of the standard H/W_{co} ratio of Etnean scoria cones allows the following conclusions:

1) We should pay attention to the method used to calculate H (relative height) of a cone located on a slope of a large volcano flank. Whereas the classical method (Settle, 1979) to obtain H will give the right result for flat or gently dipping basal planes, in the case of position on a steeper flank we should use our improved definition, i.e. H measured relative to the fitted basal plane. For Etnean cones having basal planes <5°, the two methods are roughly the same, but for steeper slopes, we will get smaller values, the error being as high as 20–30%. In other words, as a rule, the standard ratio for H/W_{co} of scoria cones on volcano flanks tend to be smaller than the ideal 0.18.
2) The smaller H/W_{co} ratios are further reduced by lava burial that is a common phenomenon on large central volcanoes such as Etna. This can be plotted better on the H_{mean}/W_{co} plot, that is, by using the mean elevation of cone instead of the classical H_{max}. Also, we have pointed out that well formed cones (i.e. regular shaped cones that are typically not affected by lava burial) have larger H/W_{co} values than other cones and, within the latter, especially the cones affected by structural deformation (i.e. double cones, rifted cones, etc.).
3) In spite of the short time span of Etna's cones, there is a trend showing progressively smaller H/W_{co} ratios for historical, old and very old cones. This trend is further supported by the progressively smaller average slope values for these cone classes, as well as the presence of erosion by gully dissection as an indication for relatively old age.

The use of high-resolution topographic data on active volcanoes is a good tool to determine the morphometric parameters of scoria cones, which in turn allows one to quantify the effect of lava burial and establish a rough relative age. Clearly, detailed field geology could provide a strong contribution to further quantification.

Acknowledgments

The research was supported by fundings from the MIUR Project 'Sviluppo Nuove Tecnologie per la Protezione e Difesa del Territorio dai Rischi Naturali' and from the Italian Dipartimento Protezione Civile to the Istituto Nazionale di Geofisica e Vulcanologia. We thank A. Tibaldi and an anonymous reviewer for their revision.

Appendix A. Supplementary data

Supplementary data associated with this article can be found, in the online version, at doi:10.1016/j.jvolgeores.2009.07.011.

References

Acocella, V., Neri, M., 2003. What makes flank eruptions? The 2001 Mount Etna eruption and its possible triggering mechanisms. Bull. Volcanol. 65, 517–529. doi:10.1007/s00445-003-0280-3.
Alderigi, P., 1998. I coni eccentrici dell'Etna: distribuzione e caratteri morfologici e chimici. Thesis, University of Pisa, Pisa, 1–147.
Allard, P., Behncke, B., D'Amico, S., Neri, M., Gambino, S., 2006. Mount Etna 1993–2005: Anatomy of an evolving eruptive cycle. Earth Sci. Rev. 78, 85–114.
Andronico, D., Branca, S., Calvari, S., Burton, M., Caltabiano, T., Corsaro, R.A., Del Carlo, P., Garfi, G., Lodato, L., Miraglia, L., Muré, F., Neri, M., Pecora, E., Pompilio, M., Salerno, G., Spampinato, L., 2005. A multi-disciplinary study of the 2002–03 Etna eruption: insights into a complex plumbing system. Bull. Volcanol. 67, 314–330.
Behncke, B., Neri, M., 2003. Cicles and trends in the recent eruptive behavior of Mount Etna (Italy). Can. J. Earth Sci. 40, 1405–1411.
Bloomfield, K., 1975. A late-Quaternary monogenetic volcano field in central Mexico. Geol. Rundsch. 64, 476–497.
Borgia, A., Ferrari, L., Pasquarè, G., 1992. Importance of gravitational spreading in the tectonic and volcanic evolution of Mount Etna. Nature 357, 231–235.
Branca, S., Del Carlo, P., 2004. Eruptions of Mt. Etna during the past 3200 years: a revised compilation integrating the historical and stratigraphic records. In: Bonaccorso, A., Calvari, S., Coltelli, M., Del Negro, C., Falsaperla, S. (Eds.), Mt. Etna: Volcano Laboratory: Geophysical Monograph Series, vol. 143, pp. 1–27.
Branca, S., Coltelli, M, Groppelli, G., 2004. Geological evolution of Etna volcano. In: Bonaccorso, A., Calvari, S., Coltelli, M., Del Negro, C., Falsaperla, S. (Eds.), Mt. Etna: Volcano Laboratory: Geophysical Monograph Series, vol. 143, pp. 49–63.
Calvari, S., Neri, M., Pinkerton, H., 2002. Effusion rate estimations during the 1999 summit eruption on Mount Etna, and growth of two distinct lava flow fields. J. Volcanol. Geotherm. Res. 119, 107–123.
Catalano, S., Torrisi, S., Ferlito, C., 2004. The relationship between Late Quaternary deformation and volcanism of Mt. Etna (eastern Sicily): new evidence from the sedimentary substratum in the Catania region. J. Volcanol. Geotherm. Res. 132, 311–334.
Chester, D.K., Duncan, A.M., Guest, J.E., Kilburn, C.R.J., 1985. Mount Etna: The anatomy of a volcano. InChapmann and Hall, London, pp. 1–404.
Coltelli, M., Del Carlo, P., Vezzosi, L., 1995. Stratigraphy of the Holocene Mt. Etna explosive eruptions. Period. Mineral. 64, 141–143.
Coltelli, M., Del Carlo, P., Vezzoli, L., 1998. The discovery of a Plinian basaltic eruption of Roman age at Etna volcano, Italy. Geology 26, 1095–1098.

Connor, C.B., Conway, F.M., 2000. Basaltic volcanic Fields. In: Sigurdsson, H. (Ed.), Encyclopedia of Volcanoes. Academic Press, New York, pp. 331–343.
Corazzato, C., Tibaldi, A., 2006. Fracture control on type, morphology and distribution of parasitic volcanic cones: an example from Mt. Etna Italy. J. Volcanol. Geotherm. Res. 158, 177–194.
Del Carlo, P., Branca, S., 1998. Tephrostratigraphic dating of the pre-1300 AD SE flank eruptions of Mt. Etna. Acta Vulcanol. 10, 33–37.
Dohrenwend, J.C., Wells, S.G., Turrin, B.D., 1986. Degradation of Quaternary cinder cones in the Cima volcanic field, Mojave Desert, California. Geol. Soc. Am. Bull. 97, 421–427.
Favalli, M., Pareschi, M.T., 2004. Digital elevation model construction from structured topographic data: the DEST algorithm. J. Geophys. Res. 109, 1–17. doi:10.1029/2004JF000150.
Favalli, M., Fornaciai, A., Pareschi, M.T., 2009. LiDAR strip adjustment: application to volcanic areas. Geomorphology 111, 123–135.
Froger, J.-L., Merle, O., Briole, P., 2001. Active spreading and regional extension at Mount Etna imaged by SAR interferometry. Earth Planet. Sci. Lett. 187, 245–258.
Garduno, V.H., Neri, M., Pasquarè, G., Borgia, A., Tibaldi, A., 1997. Geology of the NE rift of Mt. Etna (Sicily, Italy). Acta Vulcanol. 9, 91–100.
Gvirtzman, Z., Nur, A., 1999. The formation of Mount Etna as the consequence of slab rollback. Nature 401, 782–785.
Hasenaka, T., Carmichael, I.S.E., 1985. The cinder cones of Michoacán–Guanajuato, central Mexico: their age, volume and distribution, and magma discharge rate. J. Volcanol. Geotherm. Res. 25, 105–124.
Hooper, D.M., Sheridan, M.F., 1998. Computer-simulation models of scoria cone degradation. J. Volcanol. Geotherm. Res. 83, 241–267.
Kieffer, G., 1975. Sur l'existence d'une "riftzone" à l'Etna. C. R. Acad. Sci. Paris, Ser. D 280, 263–266.
Lundgren, P., Casu, F., Manzo, M., Pepe, A., Bernardino, P., Sansosti, E., Lanari, R., 2004. Gravity and magma induced spreading of Mount Etna volcano revealed by satellite radar interferometry. Geophys. Res. Lett. 31, L04602. doi:10.1029/2003GL018736.
Martin del Pozzo, A.L., 1982. Monogenetic vulcanism in Sierra Chichinautzin, Mexico. Bull. Volcanol. 45, 9–24.
Mazzarini, F., Armienti, P., 2001. Flank cones at Mount Etna Volcano: do they have a power-law distribution? Bull. Volcanol. 62, 420–430.
Mazzarini, F., Pareschi, M.T., Favalli, M., Isola, I., Tarquini, S., Boschi, E., 2005. Morphology of basaltic lava channels during the Mt. Etna September 2004 eruption from airborne laser altimeter data. Geophys. Res. Lett. 32, L04305. doi:10.1029/2004GL021815.
McGetchin, T.R., Settle, M., Chouet, B.A., 1974. Cinder cone growth modeled after Northeast Crater, Mount Etna, Sicily. J. Geophys. Res. 79, 3257–3272.
Monaco, C., Tapponier, P., Tortorici, L., Gillot, P.Y., 1997. Late quaternary slip-rates on the Acireale–Piedimonte normal fault and tectonic origin of Mt. Etna (Sicily). Earth Planet. Sci. Lett. 147, 125–139.
Moriya, I., 1986. Morphometry of pyroclastic cones in Japan. Bull. Soc. Vol. Japan 3, 58–76 (in Japanese, with English Abstr.).
Porter, S.C., 1972. Distribution, morphology, and size frequency of cinder cones on Mauna Kea volcano, Hawaii. Geol. Soc. Am. Bull. 83, 3607–3612.
Riedel, C., Ernst, G.G.J., Riley, M., 2003. Controls on the growth and geometry of pyroclastic constructs. J. Volcanol. Geotherm. Res. 127, 121–152.
Rittmann, A., 1973. Structure and evolution of Mount Etna. Philos. Trans. R. Soc. Lond. 274, 5–16 A.
Romano, R., 1982. Succession of the volcanic activity in the Etnean area. Mem. Soc. Geol. Ital. 23, 75–97.
Romano, R., Sturiale, C., 1981. Geologia del versante sud orientale etnea F°270 IV (NO, NE, SO, SE). Boll. Soc. Geol. Ital. 100, 15–40.
Romano, R., Sturiale, C., 1982. The historical eruptions of Mt. Etna (Volcanological data). Mem. Soc. Geol. Ital. 23, 75–97.
Romano, R., Sturiale, C., Lentini, F. (coordinators), 1979. Geological map of Mount Etna (scale 1:50,000). S.EL.CA. Firenze (made available in: Memorie della Società Geologica Italiana, 23, 1982).
Scott, D.H., Trask, N.J., 1971. Geology of the Lunar Crater Volcanic Field, Nye County: NV. U.S. Geol. Surv., Prof. Paper, vol. 599-I. 22 pp.
Settle, M., 1979. The structure and emplacement of cinder cone fields. Am. J. Sci. 279, 1089–1107.
Tanguy, J.-C., Condomines, M., Le Goff, M., Chilleni, V., La Delfa, S., Patanè, G., 2007. Mount Etna eruptions of the last 2750 years: revised chronology and location through archeomagnetic and 226Ra–230Th dating. Bull. Volcanol. doi:10.1007/s00445-007-0121-x.
Tarquini, S., Isola, I., Favalli, M., Mazzarini, F., Bisson, M., Pareschi, M.T., Boschi, E., 2007. TINITALY/01: a new Triangular Irregular Network of Italy. Ann. Geophys. 50, 407–425.
Tibaldi, A., 1995. Morphology of pyroclastic cones and tectonics. J. Geophys. Res. 100 (B12), 24521–24535.
Villari, L., Rasà, R., Caccamo, A., 1988. A volcanic hazard at Mt. Etna (Sicily, Italy). Some insight from the geostructural pattern constraining flank eruptions. Proc Kagoshima International Conference on Volcanoes, pp. 491–494.
Wood, C.A., 1980a. Morphometric evolution of cinder cones. J. Volcanol. Geotherm. Res. 7, 387–413.
Wood, C.A., 1980b. Morphometric analysis of cinder cone degradation. J. Volcanol. Geotherm. Res. 8, 137–160.